Hyperfunctional Parathyroid Glands with ^{99m}Tc-MIBI Scan: Semiquantitative Analysis Correlated with Histologic Findings

Shigeo Takebayashi, Hideo Hidai, Tetsuo Chiba, Yutaka Takagi, Yukio Nagatani and Sho Matsubara

Departments of Radiology and Pathology, Yokohama City University Hospital, Yokohama; and Department of Urology, Yokohama Daiichi Hospital, Yokohama, Japan

The purpose of this study was to correlate the semiquantitative analysis of ^{99m}Tc-methoxyisobutyl isonitrile (MIBI) scan with histologic findings of hyperfunctional parathyroid glands. **Methods:** Early and delayed cervical images of MIBI scans were reviewed in 31 patients who eventually underwent parathyroidectomies because of biochemically suspected hyperparathyroidism ([HPT], primary, n = 13; secondary, n = 18). The sensitivity of a scan for localizing the diseased glands was determined by comparing scan findings with pathologic findings, which were considered the gold standard. The average ratio of parathyroid-to-thyroid (P/T) count was compared between glands with large and small areas of whole gland, chief cell, oxyphil cell or cellular components. The mean areas of whole gland, chief cells and oxyphil cells were also compared between glands detected by MIBI scan and those that the scan missed. **Results:** There were 99 resected lesions, including 9 parathyroid adenomas and 61 hyperplastic parathyroids. The sensitivity for localizing the diseased glands in patients with primary HPT (91%) was higher than that in patients with secondary HPT (83%). Significantly greater average P/T counts ratio on both early and delayed images was observed in the diseased glands with greater areas of whole gland, chief cells, oxyphil cells or cellular components. Fifty-nine MIBI-positive glands had significantly greater average areas of whole gland ($P < 0.001$) and chief cell ($P = 0.002$) than did 11 MIBI-negative glands. **Conclusion:** The uptake of MIBI in hyperfunctional parathyroid is dependent on gland size and the amount of cellular components, chief cells and oxyphil cells. However, the amount of oxyphil cells does not clearly affect the results of MIBI parathyroid scintigraphy, because it is small in most hyperfunctional glands.

Key Words: ^{99m}Tc-methoxyisobutyl isonitrile; parathyroid hyperfunction; parathyroid hyperplasia; parathyroid adenoma

J Nucl Med 1999; 40:1792–1797

Localization of hyperfunctional parathyroid glands in patients with hyperparathyroidism (HPT) has been a diagnostic problem. Preoperative localization of the abnormal parathyroid gland restricts surgeons to performing only limited neck surgery rather than the full exploration traditionally performed (*1*). ^{201}Tl-technetium substraction scintigraphy has been used as a technique for such localization (*2*). The uptake mechanisms of the tracer have been postulated to be increased cellular density and vascularity or, in part, dependent on the presence of mitochondria-rich oxyphil cells (*3*).

^{99m}Tc-methoxyisobutyl isonitrile (MIBI), which is a lipophilic cationic complex, was originally introduced for myocardial perfusion studies (*4*). MIBI has biologic properties similar to ^{201}Tl and has therefore been valuable for evaluating the viability of lesions, including parathyroid adenoma and hyperplasia. MIBI takes advantage of the superior physical properties of technetium and has a higher target-to-background ratio than ^{201}Tl (*5*). It is not hampered by the motion artifacts present in ^{201}Tl-technetium substraction scintigraphy. MIBI is taken up more avidly in parathyroid adenoma or hyperplasia than in the surrounding thyroid, and, after uptake, a slower release occurs from parathyroid cells (*6*). The exact mechanisms by which MIBI accumulates in hyperfunctional parathyroid tissue is not yet clear. However, increases in both perfusion and functional activity (*7,8*) and targeting of abundant mitochondria-rich cells have been discussed as possible mechanisms (*6*).

In this study, we semiquantitatively analyzed MIBI scans of hyperfunctional parathyroid glands and correlated the findings with histopathologic findings. By using the histologic findings as the gold standard, we also investigated differences between the diseased glands detected by MIBI scan and those lesions that were missed.

SUBJECTS AND METHODS

Patient Population

Between January 1994 and March 1998, 31 patients (20 men, 11 women) with biochemically suggestive HPT underwent parathyroidectomies after MIBI scans for preoperative localization of hyperfunctional parathyroid glands. All patients also underwent sonography and MRI to localize the diseased parathyroid glands. The 31 patients, 13 with primary HPT and 18 with secondary HPT, were 20–50 y old (mean 38 y). The times between MIBI imaging and surgery ranged from 3 to 18 d (mean ± SD, 10 ± 4 d). Serum levels of intact parathyroid hormone ranged from 608 to 1246 pg/mL

Received Sep. 14, 1998; revision accepted Apr. 19, 1999.

For correspondence or reprints contact: Shigeo Takebayashi, MD, Yokohama City University Hospital, Department of Radiology, 3-46, Urafune-cho, Minami-ku, Yokohama 232, Japan.

(mean 764 ± 4 pg/mL) in patients with primary HPT and 104–2096 pg/mL (mean 502 ± 4 pg/mL) in those with secondary HPT. The 18 with secondary HPT had undergone chronic intermittent hemodialysis for 6–12 y (mean 7 ± 2 y). The criteria for parathyroidectomy, which were independent of MIBI results, were high serum levels of intact parathyroid hormone that were not responsive to vitamin D_3 therapy or severe osteodystrophy in patients with secondary HPT.

Imaging Technique

After receiving intravenous administration of 740 MBq (20 mCi) of MIBI, all patients were scanned with a gamma camera (Multi SPECT; Siemens Medical Systems, Erlangen, Germany). Planar imaging of the neck and thorax was performed at 15 min (early image) and 2 h after injection (delayed image) with the patient supine and the neck extended. The images were obtained with a low-energy, parallel-hole, high-resolution collimator and a 20% energy window centered on the 140 KeV peak. About 5×10^5 counts were recorded in each image, and digital data (256 × 256 matrix) were acquired.

Data Analysis

Both early and delayed images were reviewed for the detection of hyperfunctional parathyroid glands by two radiologists experienced in radionuclide examinations. The observers were blinded to the results of other imaging findings, operative results, pathological results, clinical histories and laboratory data. In lesions overlying the thyroid, a positive finding for hyperfunctional parathyroid gland was determined when the tracer accumulation in the lesions was separable from the residual thyroid activity on delayed image. In lesions that were apart from the thyroid, a positive finding was determined when the lesions had higher tracer activity than the residual thyroid activity on delayed image. The observers also described the prolonged activity in the thyroid on the delayed MIBI scan. The scans were read independently, and if there was disagreement, the observers discussed their findings and reached a consensus opinion.

After interpreting the MIBI images, the observers were apprised of the surgical and pathologic results. Then they analyzed the MIBI scans semiquantitatively. A 256 × 256 matrix image of MIBI was converted to a 128 × 128 image, because average counts per pixel in a 256 × 256 matrix image are too small for comparisons. Average counts of the diseased parathyroid gland and normal thyroid gland were obtained after a region of interest (ROI) was drawn manually around each area. The ROI for normal thyroid and that for MIBI false-negative parathyroid lesions were drawn in reference to the surgical findings. The parathyroid-to-thyroid (P/T) counts ratio was determined using the average counts of the diseased parathryoid glands and normal thyroid glands.

Pathologic Evaluation

All formalin-fixed parathyroid tissues were sectioned (10 μm thick) and stained with hematoxylin and eosin; then the stained sections were examined by a pathologist who did not know the results of the MIBI scans. The areas of whole gland, chief cells and oxyphil cells in the tissue were approximated with the SPICCA semiautomatic image-processor system (Nippon Avionix, Tokyo, Japan). The area of eosinophilic micronodules in the tissue was calculated on a low-power field, and the cell type of the nodules, which was suspected to be oxyphil, was confirmed on a high-power field. The area of transitional oxyphil cells, which are a variant of oxyphil cells with less invasive cytoplasmic eosinophilia than oxyphil cells, was classified as an oxyphil-cell–occupying area. The remaining areas with slight eosinophilia were classified as chief-cell–occupying areas after the cell type was confirmed. The pathologist also documented the presence of hemorrhage, fibrosis, cystic change or fatty infiltration, and scored histologic features as follows: 0 = not present; 1 = mild frequency; 2 = moderate frequency; 3 = marked frequency. Subsequently, the diseased parathyroid glands were divided into those with high cellularity (total score ≤ 3) and those with low cellularity (total score ≥ 4) after total scores were calculated in each parathyroid tissue section.

Statistical Analysis

We compared the sensitivity of a MIBI scan for localizing hyperfunctional parathyroid glands and average P/T counts ratio in glands between patients with primary HPT and those with secondary HPT. The average P/T counts ratio was also compared between the glands with large (greater than mean values) and small (less than mean values) areas of whole gland, chief cells or oxyphil cells. A similar comparison was made between high-cellular glands and low-cellular lesions. We also compared mean values of (a) whole gland areas, (b) chief cell areas, (c) oxyphil cell areas and (d) scores of cellular components between lesions detected by MIBI scan and those that were missed. Unpaired Student *t* test was used to analyze the difference with <0.05 considered as significant.

RESULTS

Primary Hyperparathyroidism

On the basis of the surgical and pathologic results, 21 nodes were resected in the 13 patients with primary HPT (Table 1). Of the 13 patients, 2 were found to have no diseased parathyroid, but they did have 2 normal juxtathyroidal lymph nodes (6 and 8 mm in size). The lymph nodes, which were interpreted as diseased parathyroid glands on

TABLE 1
Results of MIBI Scans of 99 Resected Nodes in 31 Patients with Primary and Secondary Hyperparathyroidism

	Primary HPT (13 patients)		Secondary HPT (18 patients)	
	Positive	Negative	Positive	Negative
Diseased parathyroid				
Adenoma (n = 9)	8	1	0	0
Hyperplasia (n = 47)	2	0	35	10
Adenomatous-nodular hyperplasia (n = 14)	0	0	14	0
Others				
Normal parathyroid (n = 5)	0	5	0	0
Thyroid adenoma (n = 3)	1	0	2	0
Thymus (n = 10)	0	0	0	10
Normal lymph node (n = 9)	0	4	0	5
Metastatic lymph node (n = 2)	0	0	0	2
Total (n = 99)	11	10	51	27

MIBI = methoxyisobutyl isonitrile; HPT = hyperparathyroidism.

both sonography and MRI, were negative on MIBI scan. The other 2 resected lymph nodes were negative on MIBI scan, sonography and MRI. The remaining 11 patients included 9 with solitary parathyroid adenomas and 2 with solitary parathyroid hyperplasia. Delayed MIBI scans showed prolonged thyroid activities in 5 patients (38% of the 13 patients). However, MIBI scintigraphy correctly identified and precisely localized 10 of the 11 diseased parathyroid glands (Fig. 1), including 1 juxtathyroidal lesion and 1 ectopic lesion. There was a false-positive thyroid adenoma (10 mm in size) in 1 patient with primary HPT. The sensitivity and specificity of MIBI scan for localizing hyperfunctional parathyroid glands in the patients with primary HPT were 91% and 90%, respectively.

Secondary Hyperparathyroidism

In the 18 patients with secondary HPT, 78 nodes were resected, 59 of which were hyperplastic parathyroid glands, including 14 adenomatous-nodular hyperplastic lesions (Table 1). Each of the 18 patients was found have 1 or more parathyroid hyperplasic lesions. Delayed MIBI scans showed prolonged thyroid activities in 8 patients (33%). The scans correctly identified 49 of the 59 diseased glands but missed 10 retrothyroidal hyperplastic glands (4–12 mm in size).

No correlation was found between scintigraphic localization and the anatomic location (upper versus lower and right versus left glands). A hyperplastic parathyroid gland with a large cystic degeneration did not accumulate much MIBI according to early phase scans and demonstrated washout, resulting in a negative delayed image (Fig. 2). There were two false-positive thyroid adenomas. However, the metastatic lymph nodes from an anaplastic cell carcinoma of unknown origin were correctly shown to be negative for diseased parathyroid glands on delayed MIBI scan, on which most accumulations of the lesions were washed out (Fig. 3). Surgical findings showed that these lesions were contiguous with the thyroid right lobe and parathyroid lesions, as observed on sonography and MRI, which suggested enlarged parathyroid glands. The sensitivity and specificity of the MIBI scans for localizing hyperfunctional parathyroid glands in the patients with secondary HPT were 83% and 89%, respectively.

Correlation Between Histologic and Scintigraphic Findings

The 70 diseased parathyroid glands showed high cellularity in 40 glands and low cellularity in 30 glands. All 9 adenomas evaluated contained predominantly chief cells or mixed cells. The majority of the adenomas contained solidly arranged chief cells intermingled with very few fat cells. Of the 61 hyperplastic glands, including 14 adenomatous-nodular hyperplasia, 55 (90%) contained chief cells or were mixed type, and 6 (10%) contained predominantly oxyphil cells. There were no findings of clear cell hyperplasia. Mean cell distributions in the 70 diseased glands were chief cell in 85% and oxyphil cell in 15%.

Table 2 presents the correlation of average P/T counts ratios with cellular patterns in the 70 hyperfunctional parathyroid glands. The average counts ratios were 1.28 (range 0.82–1.78; SD 0.26) for early scans and 1.42 (range 0.94–2.37; SD 0.37) for delayed scans. There was no statistically significant difference in the average counts ratio between hyperfunctional glands in patients with primary HPT and those in patients with secondary HPT. However, the counts ratios were significantly higher in high-cellular parathyroid glands than in low-cellular glands on either early or delayed scans. The glands with greater areas of either whole gland, chief cells or oxyphil cells also had significantly greater average counts ratios than those with a smaller area of each on either early or delayed images.

Table 3 lists the cellular patterns of the 70 hyperfunctional parathyroid glands and shows the differences between the 59 MIBI true-positive glands and the 11 false-negative lesions. The MIBI true-positive glands had a significantly greater mean area of either whole gland or chief cells than the area

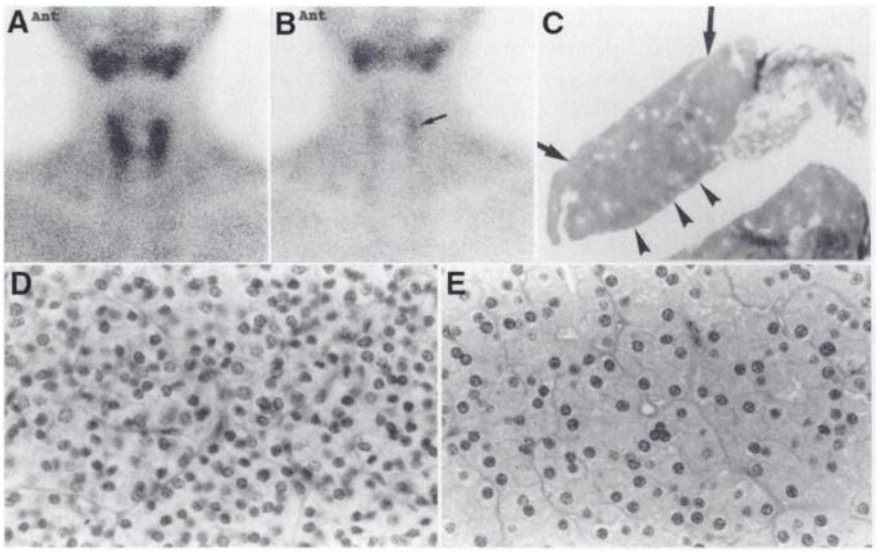

FIGURE 1. In patient with primary HPT, early MIBI scan of neck (A) shows no abnormal uptake. Delayed MIBI image (B) shows separately increased activity (arrow) in left upper quadrant of thyroid. Low-power field of 10-mm–sized parathyroid hyperplasia specimen (arrows, C) shows small micronodules of oxyphil cells (arrowheads, C). High-power field of hyperplasia specimen shows chief cells (D) and oxyphil cells with eosinophilic cytoplasms (E).

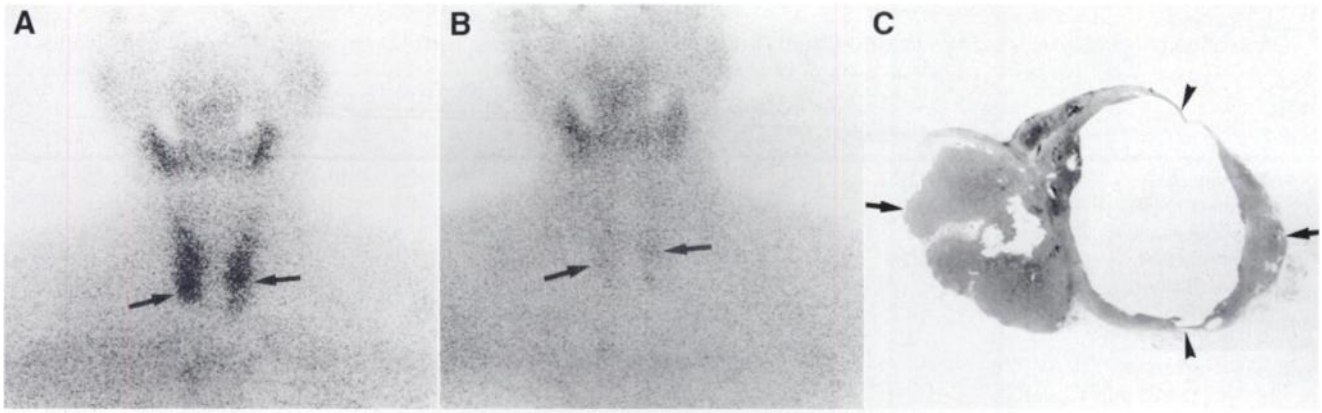

FIGURE 2. In patient with secondary HPT, early MIBI image of neck (A) shows small areas of equivocally increased uptake in left interpole and right lower pole of thyroid (arrows). However, delayed image (B) shows no separately increasing uptake in left interpole or right lower pole of thyroid (arrows) from residual thyroid activity. Low-power field of left MIBI false-negative gland specimen (23 mm in size, arrows, C) shows large area of cystic degeneration (arrowheads). MIBI false-negative hyperplasia in right lower quadrant was 13 mm in size.

in MIBI false-negative glands. The MIBI true-positive glands also had a greater mean oxyphil cells area than that in the false-negative glands, although the difference was not statistically significant. There was no significant difference in mean scoring for cellularity between the glands detected by MIBI and those that were missed.

DISCUSSION

There are two main types of parenchymal cells present in hyperfunctional parathyroid glands, chief cells and oxyphil cells. Chief cells, which are normally the active endocrine cells, have slightly eosinophilic cytoplasms containing few mitochondria. Oxyphil cells appear as isolated cells among the chief cells and form aggregates or even micronodules 1–2 mm in diameter (*9*). The oxyphil cell cytoplasm is rich in eosinophilic granules, which are numerous, tightly packed mitochondria and are thought capable of parathyroid hormone production (*10*). A transitional oxyphil cell, which is a variant of the oxyphil cell, has less invasive cytoplasmic eosinophilia than the oxyphil cell. These transitional cells are occasionally observed in parathyroid adenoma or hyperplasia. Clear cells with foamy, water-clear cell cytoplasm are fundamentally inactive cells with an unknown function (*3*).

In parathyroid glands, one cell commonly predominates, but there may be various mixtures of chief cells with oxyphil cells and transitional oxyphil cells (*9*). Primary hyperplastic parathyroid tissue also is composed of uniform chief cells or a mixture of chief cells, oxyphil cells and transitional oxyphil cells (*9*). The histopathologic patterns of secondary hyperplasia are divided into two types; diffuse type and adenomatous-nodular type (*11*). The diffuse type of hyperplasia, in which cords, sheets and follicular arrangements of the cells replace the stromal fat cells, is the classic pattern and is indistinguishable from primary hyperplasia. In adenomatous-nodular hyperplasia, however, the cells are grouped together in large islands or nodules. Although oxyphil cells are observed more frequently in diffuse hyperplasia, necrosis is observed more frequently in adenomatous-nodular hyperplasia (*12*).

Double-phase MIBI imaging represents a promising single-agent scintigraphy that does not require subtraction. The washout of MIBI from parathyroid adenoma or hyperplasia

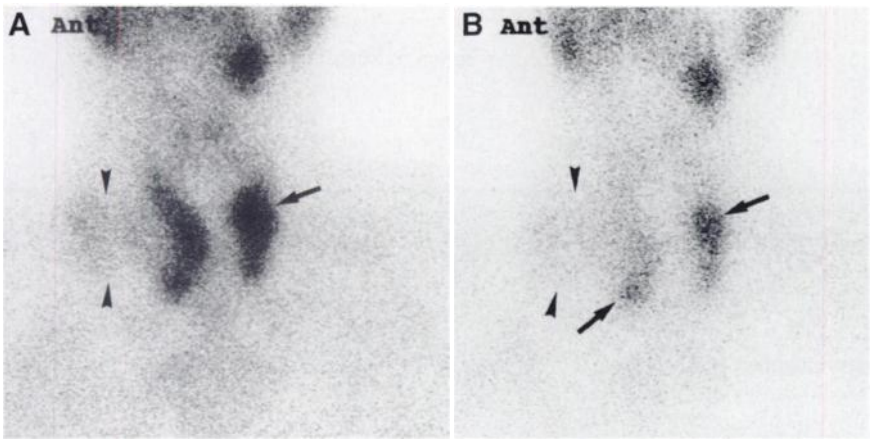

FIGURE 3. In patient with secondary HPT, early MIBI scan of neck (A) shows compression of right thyroid lobe by increased uptake (arrowheads) and focal increased tracer activity in left upper pole of thyroid (arrow). (B) Delayed MIBI scan shows most tracer activity in right neck is washed out (arrowheads) and distinguished from diseased parathyroid glands with separately increased activities (arrows) in left upper and right lower quadrants of thyroid. Lesions in right neck were two metastatic lymph nodes from anaplastic cell carcinoma of unknown origin.

TABLE 2
Correlation of Parathyroid-to-Thyroid MIBI Count Ratios with Cellular Patterns in 70 Hyperfunctional Parathyroid Glands

	No. of nodes	Average (SD) P/T count ratios			
		Early image	*P*	Delayed image	*P*
Primary HPT	11	1.27 (0.33)	NS	1.54 (0.49)	NS
Secondary HPT	59	1.28 (0.25)		1.37 (0.35)	
Low cellularity	30	1.18 (0.26)	0.005	1.27 (0.35)	0.017
High cellularity	40	1.35 (0.24)		1.49 (0.37)	
Areas of glands					
Mean (>97 mm^2)	42	1.18 (0.04)	0.0001	1.19 (0.25)	0.0002
Mean (<97 mm^2)	28	1.42 (0.04)		1.43 (0.22)	
Chief cell areas					
Mean (>85 mm^2)	48	1.23 (0.27)	0.03	1.35 (0.32)	0.017
Mean (<85 mm^2)	22	1.37 (0.22)		1.58 (0.42)	
Oxyphil cell areas					
Mean (>11 mm^2)	54	1.22 (0.26)	0.0006	1.37 (0.36)	0.030
Mean (<11 mm^2)	16	1.47 (0.16)		1.60 (0.35)	

MIBI = methoxyisobutyl isonitrile; P/T = parathyroid-to-thyroid; HPT = hyperparathyroidism; NS = not significant.

is slower than that from surrounding thyroid tissue. This differential washout constitutes the rationale for the use of MIBI for parathyroid single radiotracer scintigraphy (*13*). The uptake in diseased parathyroid glands is usually distinguishable on delayed image. However, an early MIBI scan is useful for detecting disease activity in parathyroid glands when the activity of the thyroid is prolonged on the delayed scan. The early phase scan is also useful for localization of a hemorrhagic or large hyperplastic parathyroid gland with degeneration, because it may demonstrate washout and, hence, result in a negative delayed image (*14*). Furthermore, the early phase scan is also helpful and is used as an anatomic reference to locate the abnormal focus of persistent uptakes (*13*).

MIBI scintigraphy is useful in differential diagnosis between malignancies and nonmalignant neck tumors because the malignant neoplasms have an increasing accumulation of the tracer on an early scan (*15*). Therefore, the differentiation of enlarged hyperfunctional parathyroid from malignant neoplasms or metastatic lymph nodes is necessary in lesions near the thyroid. Two types of delayed MIBI scans, retention of the tracer and washout of the tracer, have been reported in malignant neoplasms. The delayed scan is very useful for the differentiation of parathyroid from neoplasms that have washout of the tracer. This tracer washout in malignant neoplasms may be related to overexpression of cytoplasma cell membrane P-glycoproteins (*16*).

Various mechanisms explaining the MIBI accumulation in hyperfunctional parathyroid glands have been discussed. O'Doherty et al. (*6*) postulated that MIBI is trapped within mitochondria by the large negative transmembrane potential, similar to the mechanism for MIBI uptake by cardiac myocytes and fibroblasts (*17*). Their study demonstrated that this tracer is bound and retained more in diseased glands with a greater area of mitochondria-rich oxyphil cells than in those with a greater area of chief cells. However, the results of this study indicate that lesion detectability is correlated with gland size and the amount of chief cells, as well as the amount of oxyphil cells. Most parathyroid adenomas and hyperplasias in this study contained relatively few oxyphil cell, and the amounts may have been too small to have any effect on localization of the diseased glands by scan. The amount of chief cells also affects lesion detectability on scintigraphy because chief cells with few mitochondria

TABLE 3
Cellular Patterns of 70 Hyperfunctional Parathyroid Glands Compared Between MIBI True-Positive Lesions and False-Negative Lesions

	True-positive glands mean ± SD (range) (n = 59)	False-negative glands mean ± SD (range) (n = 11)	*P*
Whole gland areas (mm^2)	113.3 ± 85.8 (27.6–391.1)	20.5 ± 9.6 (11.1–32)	<0.001
Chief cell areas (mm^2)	99.2 ± 87.6 (13.8–386.5)	18.6 ± 8.9 (9.6–27.6)	0.002
Oxyphil cell areas (mm^2)	13.2 ± 27.9 (0–137.2)	1.4 ± 1.9 (0–4.9)	NS
Total scores for cellularity*	3.5 ± 1.6 (1–8)	3.3 ± 1.9 (0–6)	NS

*Score for cellularity: hemorrhage, fibrosis, cystics change, fatty infiltration. 0 = not present; 1 = mild frequency; 2 = moderate frequency; 3 = marked frequency.
MIBI = methoxyisobutyl isonitrile; NS = not significant.

occupy large areas of most parathyroid adenomas or hyperplastic glands.

The distribution of MIBI in vivo not only represents metabolic function but also is a simple function of blood flow. Gland size (weight) and gland vascularity are significant predictors of MIBI uptake, and they are most likely to correlate with increased delivery and, consequently, with increased accumulation of radiotracer in an abnormal gland (*18*). Dynamic MIBI images and color Doppler sonography were both successful in demonstrating increased vascularity in a region of an autograft of a parathyroid (*7*). The location of hyperfunctional glands is apparently another factor influencing lesion detectability, because a MIBI scan easily detects lesions of juxtathyroidal and ectopic parathyroid glands. The sensitivity for localizing hyperfunctional parathyroid gland in patients with secondary HPT (55%–83%) was reported to be lower than in patients with primary HPT (89%–98%) (*6,13,18–20*). Investigators have speculated that MIBI uptake, such as ^{201}Tl, in parathyroid glands is reduced in patients with chronic renal failure as a result of the interference of several factors present in uremia (*3*). However, we found no significant difference in the uptake of MIBI in diseased glands between primary HPT and secondary HPT. One reason for the higher sensitivity in patients with primary HPT is the high incidence of adenomas. The most frequent pattern is characterized histologically as parathyroid adenomas of high cellularity that lack degenerative or hemorrhagic changes. In parathyroid hyperplasia, however, there are variable pathologic features, such as necrotic degeneration, cystic transformation, calcification and fatty infiltration. Localization may be impaired in low-cellular hyperplastic glands. The occurrence of multiple parathyroid lesions is another important factor in the low sensitivity for localizing diseased glands in patients with secondary HPT. An observer has difficulty in distinguishing increased uptake in each quadrant of the thyroid in multiple hyperplastic glands in which one dominant gland can be interpreted as single lesion (*21*).

CONCLUSION

There was no significant difference in the uptake of MIBI between the diseased glands of patients with primary HPT and those of patients with secondary HPT. The uptake of MIBI in hyperfunctional parathyroid is dependent on the amounts of chief cells, mitochondria-rich oxyphil cells and cellular components, as well as gland size. However, the amount of oxyphil cells does not clearly affect the results of MIBI parathyroid scintigraphy because this amount is small in most hyperfunctional glands.

REFERENCES

1. Rossitch JC, Cowan RJ, Ellis MB, Griffith RF. ^{99m}Tc sestamibi for detection of parathyroid adenoma. Comparison of single and dual tracer imaging. *Clin Nucl Med.* 1995;20:220–221.
2. Winzelberg GG, Hydowitz JD, O'Hara KR, et al. Parathyroid adenomas evaluated by ^{201}Tl/^{99m}Tc pertechnetate subtraction scintigraphy and high-resolution ultrasonography. *Radiology.* 1985;155:231–235.
3. Sandrock D, Merino MJ, Norton JA, Neumann RD. Ultrastructural histology correlates with results of thallium-201/technetium-99m parathyroid subtraction scintigraphy. *J Nucl Med.* 1993;34:24–29.
4. Baillet GY, Mena IG, Kuperus JH, Robertson JM, French WJ. Simultaneous technetium-99m-MIBI angiography and myocardial perfusion imaging. *J Nucl Med.* 1989;30:38–44.
5. Staudenherz A, Telfeyan D, Steiner E, Niederle B, Leitha T, Kletter K. Scintigraphic pitfalls in giant parathyroid glands. *J Nucl Med.* 1995;36:467–469.
6. O'Doherty MJ, Kettle AG, Wells P, Collins REC, Coakley AJ. Parathyroid imaging with technetium-99m-sestamibi: preoperative localization and tissue uptake studies. *J Nucl Med.* 1992;33:313–318.
7. Chen CC, Premkumar A, Hill SC, Skarulis MC, Spiegel AM. ^{99m}Tc sestamibi imaging of a hyperfunctioning parathyroid autograft with Doppler ultrasound and MRI correlation. *Clin Nucl Med.* 1995;20:222–225.
8. Piga M, Bolasco P, Satta L, et al. Double-phase parathyroid technetium-99m-MIBI scintigraphy to identify functional autonomy in secondary hyperparathyroidism. *J Nucl Med.* 1996;37:565–569.
9. Ellis HA. Parathyroid glands. In: McGee JO, Isaacson PG, Wright NA, eds. *Oxford Textbook of Pathology.* Vol 2. Oxford, UK: Oxford University Press; 1992:1959–1968.
10. Wolpert HR, Vickery AL, Wang CA. Functioning oxyphil cell adenomas of parathyroid gland. A study of 15 cases. *Am J Surg Pathol.* 1989;13:500–504.
11. Castleman B, Roth SI. Chief-cell hyperplasia. In: Castleman B, Roth SI, eds. *Atlas of Tumor Pathology, Tumors of the Parathyroid Glands.* Washington, DC: Armed Forces Institute of Pathology; 1977:54–67.
12. Takagi H, Tominaga Y, Uchida K, et al. Polymorphism of parathyroid glands in patients with chronic renal failure and secondary hyperparathyroidism. *Endocrinol Jpn.* 1983;30:463–468.
13. Taillefer R, Boucher Y, Potvin C, Lambert R. Detection and localization of parathyroid adenomas in patients with hyperparathyroidism using a single radionuclide imaging procedure with technetium-99m-sestamibi (double-phase study). *J Nucl Med.* 1992;33:1801–1807.
14. Benard F, Lefebvre B, Beuvon F, Langlois MF, Bisson G. Rapid washout of technetium-99m-MIBI from a large parathyroid adenoma. *J Nucl Med.* 1995;36:241–243.
15. Leitha T, Glaser C, Pruckmayer M, et al. Technetium-99m-MIBI in primary and recurrent head and neck tumors: contribution of bone and SPECT image fusion. *J Nucl Med.* 1998;39:1166–1171.
16. Taki J, Sumiya H, Asada N, Ueda Y, Tsuchiya H, Tonami N. Assessment of P-glycoprotein in patients with malignant bone and soft tissue tumors using technetium-99m-MIBI scintigraphy. *J Nucl Med.* 1998;39:1179–1184.
17. Chiu ML, Kronange JF, Piwnica-Worms D. Effect of mitochondrial and plasma-membrane potentials on accumulation of hexakis (2-methoxy-isobutylisonitrile) technetium in cultured mouse fibroblasts. *J Nucl Med.* 1990;31:1646–1653.
18. Lee VS, Spritzer CE, Coleman RE, Wilkinson RH Jr, Coogan AC, Leight GS Jr. The complementary roles of fast spin-echo MR imaging and double-phase ^{99m}Tc-sestamibi scintigraphy for localization of hyperfunctioning parathyroid glands. *AJR.* 1996;167:1555–1562.
19. Chesser AM, Carroll MC, Lightowler C, MacDougall IC, Britton KE, Baker IR. Technetium-99m-methoxy isobutyl isonitrile (MIBI) imaging of the parathyroid glands in patients with renal failure. *Nephrol Dial Transplant.* 1997;12:97–100.
20. Krubsack AJ, Wilson SD, Lawson TL, et al. Prospective comparison of radionuclide, computed tomographic, sonographic and magnetic resonance localization of parathyroid tumors. *Surgery.* 1988;106:639–644.
21. Gordon BM, Gordon L, Hoang K, Spicer KM. Parathyroid imaging with ^{99m}Tc-sestamibi. *AJR.* 1996;167:1563–1568.